

Measurement of thermal conductivity of individual multiwalled carbon nanotubes by the 3- ω method

Tae Y. Choi and Dimos Poulikakos^{a)}

Laboratory of Thermodynamics, Institute of Energy Technology, ETH Zurich, CH-8092 Zurich, Switzerland

Joy Tharian and Urs Sennhauser

Electronics/Metrology Laboratory, Swiss Federal Laboratories for Materials Testing and Research, CH-8600 Duebendorf, Switzerland

(Received 1 February 2005; accepted 17 May 2005; published online 29 June 2005)

The thermal conductivity of individual multiwalled carbon nanotubes (outer diameter of ~ 45 nm) was obtained by employing the 3- ω method. To this end, the third-harmonic amplitude as a response to the applied alternate current at fundamental frequency (ω) is expressed in terms of thermal conductivity. A microfabricated device composed of a pair of metal electrodes $1 \mu\text{m}$ apart is used to place a single nanotube across the designated metal electrodes by utilizing the principle of dielectrophoresis. The multiwalled carbon nanotube was modeled as a one-dimensional diffusive energy transporter and its thermal conductivity was measured to be 650–830 W/mK at room temperature. © 2005 American Institute of Physics. [DOI: 10.1063/1.1957118]

Since the discovery of carbon nanotubes (CNTs),¹ many researchers directed their efforts to understand and characterize their unique properties. These researches have reported remarkable electrical,² mechanical,³ and thermal⁴ properties related to their unique structure and small size, making them the ideal material for various engineering applications, such as sensors,⁵ actuators,⁶ energy storage systems,⁷ and nanoelectronics.⁸ Of particular interest in this letter is the thermal conductivity of CNTs.

Thermal conductivity of single-walled CNTs was theoretically predicted to be higher than that of monocrystalline diamond.^{4,9} There have been a few attempts to measure thermal conductivity of single-walled CNT bundles.^{10–12} One study showed that the measured values of thermal conductivity were at around 30 W/mK, which is two orders of magnitude lower than the theoretically predicted value.¹⁰ These drastically reduced values result from the boundary phonon scattering between individual nanotubes in the bundle. It is difficult to measure the correct thermal conductivity due to the uncertainty of the thermal resistance in the tube-tube junctions and the filling factor of CNTs in the bundles. Therefore, it is desirable and necessary to investigate individual CNTs in order to achieve accurate and reliable data.

Thermal conductivity of a single multiwall CNT (MWCNT) has been measured, by using an indirect thermal conductance technique.¹³ A microfabricated device was used to place a single nanotube for thermal conductivity measurement. A precisely fabricated microstructure was needed for the accurate estimation of the heat flow to the substrate and to the test section. The 3- ω method proposed herein is another viable technique for the thermal property measurements of individual CNTs. So far, only the thermal conductivity of CNT bundles has been measured with the 3- ω method,¹² indicating values of order 10 W/mK for as-grown single-wall CNT bundles.

In the present work, a microfabricated device was used for the placement of individual nanotubes, which were sus-

ended between the metal electrodes. By applying an alternate current (ac) to the CNT, the third-harmonic amplitude was measured, giving rise to its thermal conductivity by the 3- ω method. The 3- ω method has been extensively used for measuring thermal conductivities of thin films and superlattices.^{14,15} In these studies, a metal pattern serving as a heater and thermometer was fabricated on a film. Due to the heat transfer to the film, the metal pattern was heating the film and sensing the temperature fluctuation at the same time. Unlike in these references, in this letter, the measurement of thermal conductivity of a single CNT was performed by using a self-heating 3- ω method. If the two ends of the CNT are in excellent thermal and electrical contact with a substrate and the nanotube in-between is suspended in a vacuum forming a bridge structure, a constant-amplitude ac current of the form $I_0 \sin \omega t$ applied through the nanotube will create a temperature fluctuation at 2ω , which will induce the third-harmonic voltage signal.¹⁶

A recent electrostatic microscopy study suggested that MWCNTs are diffusive conductors.¹⁷ For MWCNTs, heat dissipation along the nanotube is likely to occur if they are diffusive. One study estimated the temperature distribution along the tube by the scanning thermal microscopy technique, indeed showing the diffusive nature of MWCNTs.¹⁸ In this case, the one-dimensional heat diffusive equation along the tube can be utilized to obtain a closed-form solution of the third harmonic response to an accuracy of 1/81 as shown in the following equation:¹⁶

$$V_{3\omega, \text{rms}} \cong \frac{\sqrt{2} I_0^3 R R' L}{\pi^4 \kappa S}, \quad \tan \varphi = \frac{2\omega L^2}{\pi^2 \alpha}, \quad (1)$$

where R , L , S , and κ are the resistance, length, cross-sectional area, and thermal conductivity of the CNT, respectively. R' is the temperature gradient of the resistance at room temperature defined as $(dR/dT)_{T_0}$, φ and α are the phase lag of the 3- ω signal and the thermal diffusivity of CNT. This equation is valid only for low current ($< 100 \mu\text{A}$) and frequency (< 1 kHz).

^{a)} Author to whom correspondence should be addressed; electronic mail: dimos.poulikakos@ethz.ch

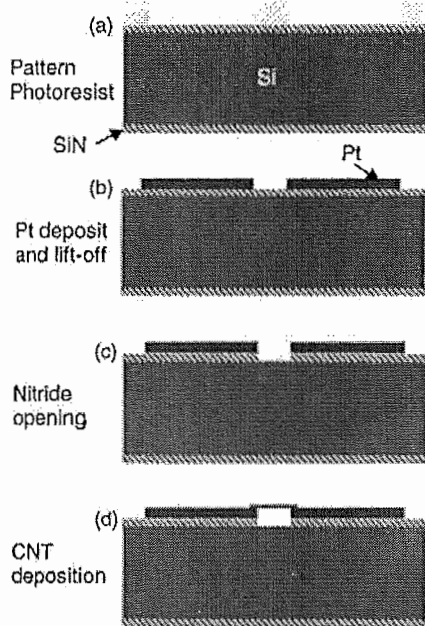


FIG. 1. The fabrication process flow for metal electrodes across which a single CNT is deposited. (a) Photoresistive pattern by light lithography, (b) Pt lift off, (c) RIE to define the trench between the electrodes, and (d) selective deposition of CNTs by dielectrophoresis.

To investigate an individual CNT, a microdevice had to be developed and fabricated using microelectromechanical system technology to place the CNT across the designated metal electrodes, which had been patterned by a two-mask lithography process (Fig. 1). An ultraviolet-lithography step can generate a photoresist (PR) pattern [Fig. 1(a)]. After thin-film evaporation of Pt on this PR patterned wafer, a lift-off process follows to define the metal electrode pattern [Fig. 1(b)]. The grown or deposited nanotubes had to be suspended between the electrodes to avoid heat loss from the nanotube to the substrate [Fig. 1(d)]. Thus, the removal of SiN layer by reactive ion etching (RIE) is necessary as a final fabrication step [Fig. 1(c)].

A droplet of solution containing commercially available MWCNTs (NanoLab) was dropped on a microfabricated chip [one of eight small chips mounted on a ceramic packaging shown in Fig. 2(a)]. Subsequently, a high-frequency (5 MHz) ac field was applied across the electrodes. Figure 2(a) shows a simple setup composed of a resistor, a capacitor, a sample, and a Teflon circuit board (the power source is

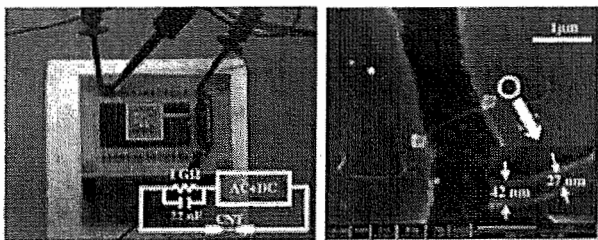


FIG. 2. Selective deposition of a single CNT across the metal electrodes and subsequent soldering by EB. (a) Equivalent circuit diagram for selective deposition and (b) soldered result by EB. The inserted picture shows a magnified view of the nanotube with ultrahigh resolution (0.6 nm resolution).

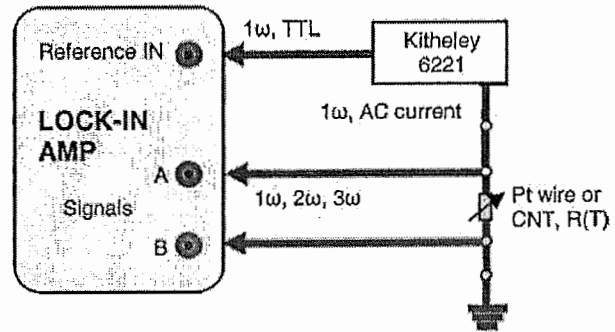


FIG. 3. Schematic diagram of measurement setup. The third-harmonic signal generated in the specimen is measured, due to the fundamental ac current excitation.

not visible in the picture). The inserted diagram represents an equivalent electric circuit. In this case, a nonuniform electric field induces dielectrophoresis¹⁹ and guides discrete CNTs in the solution to the designated electrodes. A combined use of electric fields with an ac:direct current(dc) ratio of 2:1 was used to place a single CNT across the electrodes. This combination of ac and dc takes advantage of the influence of both ac and dc during the deposition.²⁰ This selective deposition technique allows one to control the placement of single nanotubes acceptably well, as shown in Fig. 2(b).

The nanotube and the substrate are in line contact which yields a very high electrical contact resistance of the order of 1 MΩ. The resistance at the contacts must be minimized for two reasons. First, for high contact resistance, the boundary conditions will be changed and Eq. (1) is no longer valid. Second, a spurious $3-\omega$ signal can appear at very low current amplitude. To supply an electric field, with which one can measure electrical and thermal properties, a good contact must be assured. To realize this, we utilized electron-beam (EB) deposition at the nanotube-substrate contacts and subsequent annealing of the sample.

In the EB technique, one can use Pt vapor as a depositing source on top of the tube-substrate contact region as shown in Fig. 2(b). By exposing the tube-metal contact to an EB in the presence of metalorganic vapor (trimethyl cyclopentadienyl platinum, $C_9H_{16}Pt$) emitted inside an ultrahigh vacuum chamber, we were able to pattern Pt on the contact area. The metal deposits greatly enlarge the contact area between the tube and the metal contact, which reduces the electrical and thermal resistance at the contacts significantly.

The basic elements of the $3-\omega$ measurement scheme are shown in Fig. 3. Two major components, the lock-in amplifier (Stanford Research System SR850) and the constant-amplitude current source (Kithley 6221), are shown in the diagram. The lock-in amplifier can pick up the third-harmonic signal across the tube, which contains valuable thermal transport data. Assuming that the driving frequency is 1 kHz and thermal diffusivity (α) is 10^{-4} m²/s, the phase is predicted from Eq. (1) to be less than 10^{-3} degree, which is smaller than the noise level. Therefore, at the low-frequency region (below 1 kHz), one can only obtain the thermal conductivity since the thermal time constant ($L^2/\pi^2\alpha$) for a CNT is extremely small. In this frequency region, the amplitude becomes independent of the phase as shown in Eq. (1).

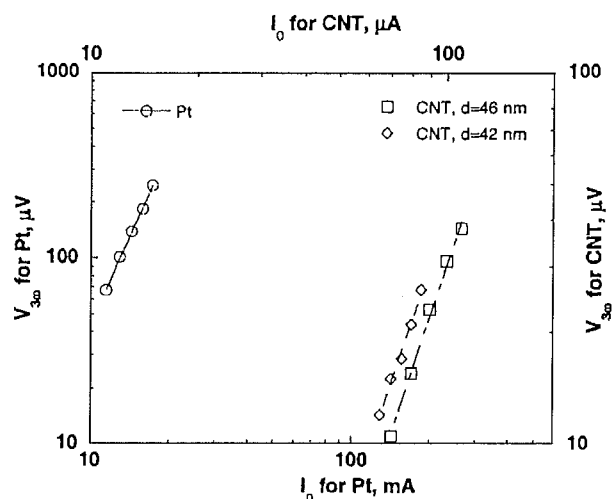


FIG. 4. 3ω amplitude as a function of current. The exponents, 2.8 and 2.9, are very close to the predicted third power, which implies the heat dissipation along the MWCNT. By fitting the result according to Eq. (1), the thermal conductivity can be obtained at 650–830 W/mK at room temperature.

To check the validity of the method, we performed a set of preliminary feasibility measurements for a platinum microwire (20 microns in diameter and 6 mm in length). The wire has four contacts and is suspended in a vacuum (1.0×10^{-2} mbar) without touching the substrate. In order to have an ideal heat sink, a sapphire substrate was used and the boundary condition was set to be at constant temperature at the contacts. The measured values are within 5% of the literature values.

The third-harmonic voltage measurement data for two suspended MWCNTs are shown in Fig. 4. The nanotube samples were annealed at 600 °C after EB deposition. The annealing process was carried out in order to minimize the electrical contact resistance. The practical elimination of this resistance was recognized as an important factor to the accurate results. Evidence toward this end was collected by measuring the total resistance ($R_{\text{total}} = R_{\text{contact}} + R_{\text{CNT}}$) of the sample with different CNT lengths and diameters prepared at the same conditions by utilizing the two-point probe technique. The lead resistance was measured at 132 Ω and not included in the total resistance. The total resistance was directly proportional to the length of the nanotube and inversely proportional to the cross-sectional area, which implies negligible contact resistance. The physical reason for this was the removal of the voids between the nanotube and metal substrate during the annealing process.²¹ The resistance and the temperature coefficient for two CNTs were measured at 296 K. The first sample with $d_{\text{outer}} = 46$ nm, $d_{\text{inner}} = 27$ nm, and $L = 1.0$ microns measured at $R = 922 \Omega$ and $R' = 1.15 \Omega/\text{K}$. The second sample ($d_{\text{outer}} = 42$ nm, $d_{\text{inner}} = 26 \pm 1$ nm, and $L = 1.1$ microns) turned out to be $R = 1320 \Omega$ and $R' = 1.39 \Omega/\text{K}$. By fitting these results according to Eq. (1), the exponent of the current amplitude I_0 was found to be 2.9 and 2.8 for the first and second sample, respectively. These values are very close to the third power

predicted from theory, a finding supporting the diffusive nature of heat transport of MWCNTs. For comparison, the exponent found for the Pt wire was 3.1. The thermal conductivity was then calculated with Eq. (1) and found to be equal to 650 and 830 W/mK for the first and second sample, respectively. Considering the two major sources of uncertainty in the measurement as the diameter of CNTs (0.6 nm resolution) and the 3ω voltage (0.5 μV resolution), we estimated the measurement error at $\pm 6\%$. The difference in the thermal conductivity between the two cases reported herein is possibly due to the size of CNTs. It should be noted that no 3ω signal solely by the lead resistance (metal electrode) was observed.

In summary, we used the 3ω method to measure the thermal conductivity of individual MWCNTs. The technique required the placement of individual nanotubes across the designated metal electrodes and EB-assisted deposition of Pt on the nanotube-metal contacts, followed by annealing. The thermal conductivity measured by this technique was found to be equal to 650 and 830 W/mK. The MWCNTs exhibited the diffusive nature of energy transport since the third-harmonic amplitude is nearly proportional to the third power of the applied current amplitude.

The authors are very grateful to Dr. H. Sehr for nitride wafers prepared in the Laboratory for Micro- and Nanotechnology of Paul Scherrer Institute, Villigen, Switzerland

¹S. Iijima, *Nature (London)* **354**, 56 (1991).

²S. Frank, P. Poncharal, Z. L. Wang, and W. A. Heer, *Science* **280**, 1744 (1998).

³E. Wong, P. E. Sheehan, and C. M. Lieber, *Science* **277**, 1971 (1997).

⁴S. Berber, Y. Kwon, and D. Tomanek, *Phys. Rev. Lett.* **84**, 4613 (2000).

⁵S. Ghosh, A. K. Sood, and N. Kumar, *Science* **299**, 1042 (2003).

⁶R. H. Baughman, C. Cui, A. Zakhidov, Z. Iqbal, J. N. Barisci, G. M. Spinks, G. G. Wallace, A. Mazzoldi, D. De Rossi, A. G. Rinzler, O. Jaschinski, S. Roth, and M. Kertesz, *Science* **284**, 1340 (1999).

⁷E. Frackowiak and F. Beguin, *Carbon* **40**, 1771 (2002).

⁸J. P. Clifford, D. L. John, L. C. Castro, and D. L. Pulfrey, *IEEE Trans. Nanotechnol.* **3**, 281 (2004).

⁹J. Che, T. Cagin, and W. A. Goddard III, *Nanotechnology* **11**, 65 (2000).

¹⁰J. Hone, M. Whitney, C. Piskoti, and A. Zettl, *Phys. Rev. B* **59**, R2514 (1999).

¹¹J. Hone, M. C. Llaguno, M. J. Biercuk, A. T. Johnson, B. Batlogg, Z. Benes, and J. E. Fischer, *Appl. Phys. A: Mater. Sci. Process.* **74**, 339 (2002).

¹²W. Yi, L. Lu, Z. Dian-Lin, Z. W. Pan, and S. Xie, *Phys. Rev. B* **59**, R9015 (1999).

¹³P. Kim, S. Li, A. Majumdar, and P. L. McEuen, *Physica B: Condensed Matter* **323**, 67 (2002).

¹⁴D. G. Cahill, *Rev. Sci. Instrum.* **61**, 802 (1990).

¹⁵S. T. Huxtable, A. R. Abramson, C. Tien, A. Majumdar, C. LaBounty, X. Fan, G. Zeng, J. E. Bowers, A. Shakouri, and E. T. Croke, *Appl. Phys. Lett.* **80**, 1737 (2002).

¹⁶L. Lu, W. Yi, and D. L. Zhang, *Rev. Sci. Instrum.* **72**, 2996 (2001).

¹⁷A. Bachtold, M. S. Fuhrer, S. Plyasunov, M. Forero, E. H. Anderson, A. Zettl, and P. McEuen, *Phys. Rev. Lett.* **84**, 6082 (2000).

¹⁸S. Li, Ph.D. thesis, University of California at Berkeley, 2001.

¹⁹X. Q. Chen, T. Saito, H. Yamada, and K. Matsushige, *Appl. Phys. Lett.* **78**, 3714 (2001).

²⁰J. Chung, K. Lee, J. Lee, and R. S. Ruoff, *Langmuir* **20**, 3011 (2004).

²¹V. Gopal, V. R. Radmilovic, C. Daraio, S. Jin, P. Yang, and E. A. Stach, *Nano Lett.* **4**, 2059 (2004).

